SUPPORTING INFORMATION

A Two-Coordinate Nickel Imido Complex that Effects C-H Amination

Carl A. Laskowski, Alexander J. M. Miller, Gregory L. Hillhouse, and Thomas R. Cundari

TABLE OF CONTENTS Page

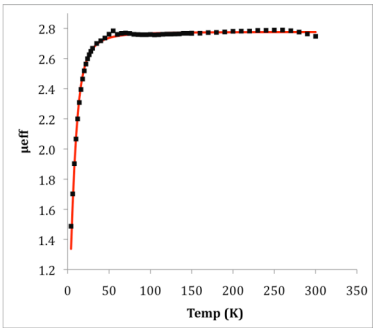

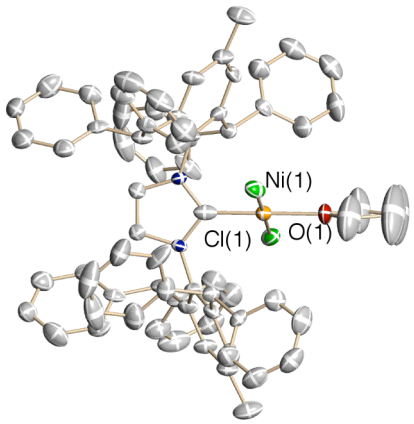

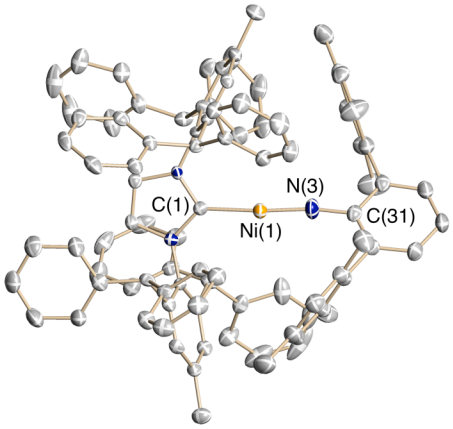

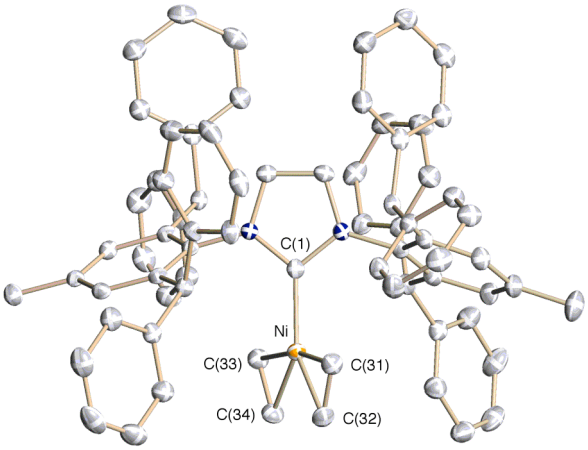

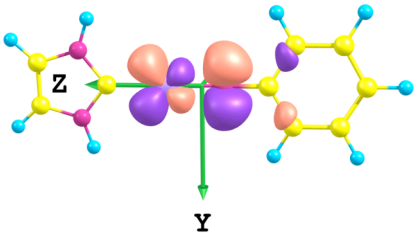

(I) Experimental Procedures

General Considerations.

Unless stated otherwise, all operations were performed in an MBraun *Lab Master* dry box under an atmosphere of purified nitrogen (*1*). Anhydrous diethyl ether was purchased from Fischer, stirred over sodium metal, and filtered through activated alumina. Pentane was purchased from Sigma Aldrich and dried by passage through activated alumina and Q-5 columns. C_6D_6 was purchased from Cambridge Isotope Laboratories, degassed by freeze-pump-thaw cycles, and dried over CaH_2 or activated 4 Å molecular sieves. Celite and 4 Å molecular sieves were activated by evacuation overnight at 180°C. IPr* (IPr* = 1,3-bis(2,6-bis(diphenylmethyl)-4-methylphenyl)imidazol-2-ylidene) and N_3(dmp) (dmp = 2,6-dimesitylphenyl) were prepared according to the literature (*2,3*). All other chemicals were used as received. Elemental analysis were performed by Midwest Microlab (Indianapolis, IN). ^{1}H NMR spectra were recorded on a Bruker 500 MHz NMR spectrometer and reported with reference to solvent resonance (residual C_6D_5H in C_6D_6, 7.16 ppm). X-ray diffraction data were collected on a Siemens Platform goniometer with a Charged Coupled Device (CCD) detector. Structures were solved by direct or Patterson methods using the SHELXTL (version 5.1) program library (G. Sheldrick, Bruker Analytical X-ray Systems, Madison, WI).

(IPr*)(THF)NiCl$_2$. IPr* (1.80 g, 1.97 mmol) and (dme)$NiCl_2$ (dme = 1,2-dimethoxyethane, 433 mg, 1.97 mmol) were combined with 20 mL THF. The solution was stirred at room temperature for 8 hours before being filtered through Celite. The purple solution was then reduced to 4 mL under vacuum. 16 mL pentane was then added to induce precipitation of fine, pale lavender solid. The solid was collected on a porous glass frit and washed with Et_2O (2 x 20 mL) to afford 2.02 g (92% yield) (IPr*)(THF)$NiCl_2$. Single crystals were grown from vapor diffusion of pentane into a THF solution of (IPr*)(THF)$NiCl_2$.

For (IPr*)(THF)$NiCl_2$: ^{1}H NMR (500 MHz, THF-d_8, 22°C): δ 7.67 (t. 8H, J = 7.0 Hz), 7.58 (t, 4H, J = 7.0 Hz), 7.42 (br, $\Delta_{½}$ = 40 Hz, 2H, HC=CH), 7.38 (d, 8H, 7.0 Hz), 6.47 (t, 4H, J = 7.0 Hz), 6.31 (br, $\Delta_{½}$ = 20 Hz, 8H), 5.44 (br, $\Delta_{½}$ = 20 Hz, 8H), 4.74 (s, 4H), 3.61 (m, 4H, THF), 1.79 (m, 4H, THF), 1.21 (s, 6H, CH_3-C_6H_2). ^{13}C{^{1}H} NMR (126 MHz, THF-d_8, 22°C): δ 192.1, 146.9, 144.2, 138.0, 132.7, 131.6, 130.9, 129.9, 128.3, 128.1, 127.7, 126.2, 68.4, 53.8, 26.8, 20.1. Anal. Calcd. for $C_{74}Cl_2H_{68}N_2NiO$: C, 78.64%; H, 5.79%; N, 2.51%. Found: C, 78.51%; H, 6.00%; N, 2.20%.

(IPr*)Ni(η^6-C_7H_8) (**1**). (IPr*)(THF)$NiCl_2$ (1.00 g, 0.896 mmol) was combined with excess Mg turnings (0.600 g) in 20 mL 1:1 THF/toluene. The slurry was stirred at room temperature for 4 hours over which time the color changed from pale lavender to black/brown before becoming a dark wine red. Solvent was removed under vacuum and the remaining red/black solid extracted with 20 mL toluene. The toluene extract was filtered through celite and dried under reduced pressure. Trituration with 2 x 15 mL Et_2O afforded 590 mg (60% yield) **2** as rust red powder.

For **1**: ^{1}H NMR (500 MHz, C_6D_6, 22°C): δ 7.62 (d, 8H, J = 7.4 Hz), 7.21 (t, 8H, J = 6Hz), 7.09-7.06 (m, 8H), 6.9-6.7 (m, 20H), 5.64 (s, 4H, -$CHPh_2$), 5.02 (s, 2H, HC=CH), 2.04 (s, 3H, CH_3-C_6H_5), 1.86 (s, 6H, CH_3-C_6H_2). $^{13}C\{^1H\}$ NMR (126 MHz, C_6D_6, 22°C): δ 194.5, 145.0, 144.8, 142.4, 138.7, 137.9, 130.8, 129.8, 129.4, 128.4, 128.2, 126.8, 126.3, 120.0, 52.0, 21.5. Anal. Calcd. for $C_{76}H_{64}N_2Ni$: C, 85.95%; H, 5.89%; N, 2.64%. Found: C, 85.46%; H, 6.07%; N, 2.63%.

(IPr*)Ni=N(dmp) (**2**). Solutions of **1** (450 mg, 0.423 mmol in 5 mL toluene) and N_3(dmp) (150 mg, 0.423 mmol in 12 mL toluene) were cooled to -35°C. While stirring, N_3(dmp) was added to **1**, causing a gradual color change from red to yellow/brown. The reaction was allowed to warm to room temperature and stirred for an additional hour. After filtration through celite, solvent was removed under reduced pressure. The resulting solid was triturated with 20 mL Et_2O and 451 mg (82% yield) **2** was collected on a porous glass frit as a fine olive-green powder. Single crystals were grown from a concentrated Et_2O solution at -35°C.

For **2**: ^{1}H NMR (500 MHz, C_6D_6, 22°C): δ 24.6 (br, $\Delta_{½}$ = 135 Hz), 15.0 (br, $\Delta_{½}$ = 290 Hz), 10.6 (br, $\Delta_{½}$ = 40 Hz), 9.35, 9.18 (br, $\Delta_{½}$ = 80 Hz), 9.08 (br, $\Delta_{½}$ = 30 Hz), 8.72 (br, $\Delta_{½}$ = 22 Hz), 6.21 (br, $\Delta_{½}$ = 74 Hz), 6.08 (br, $\Delta_{½}$ = 22 Hz), 5.06 (br, $\Delta_{½}$ = 475 Hz), 4.31, -7.58 (br, $\Delta_{½}$ = 38 Hz). Anal. Calcd. for $C_{93}H_{81}N_3Ni$: C, 85.97%; H, 6.28%; N, 3.23%. Found: C, 85.92%; H, 6.43%; N, 3.09%.

Reaction of 2 with CO. Complex **2** (146 mg, 0.112 mmol in 20 mL THF) was placed in a Schlenk flask with stirbar and cooled to -78°C. CO (11 mL, 0.454 mmol) was added via syringe, causing a color change from yellow-brown to dark red. The reaction was warmed to room temperature over which time it became colorless. After stirring for an additional 30

minutes at room temperature, solvent was removed under vacuum. The solid was extracted with 20 mL pentane and collected on a porous glass frit. The extract was dried under reduced pressure to yield 30 mg (75% yield) dmpNCO as a colorless solid. The solid from the frit, (IPr*)Ni(CO)$_3$ (**3**), was collected in 62% yield after recrystallization from CH_2Cl_2/pentane.

For dmpNCO: ^{1}H NMR (22°C, 500 MHz, C_6D_6): δ 6.98 (t, 1H, J = 8.3 Hz, C_6H_3), 6.90 (d, 2H, J = 8.3 Hz, C_6H_3), 6.87 (s, 4H, C_6H_2), 2.17 (s, 6H, p-Mes$_{dmp}$), 2.05 (s, 12H, m-Mes$_{dmp}$). ^{13}C{^{1}H} NMR (126 MHz, C_6D_6, 22°C): δ 137.7, 137.5, 136.2, 135.6, 129.4, 128.8, 128.2, 126.2, 21.1, 20.3. IR (CaF_2/Fluorolube): 2283, 2253 cm^{-1}. GC-MS (m/z) = 355.1 (M^+), 340.4.

For **3**: ^{1}H NMR (22°C, 500 MHz, CD_2Cl_2): δ 7.32-7.27 (m, 8H), 7.25-7.19 (m, 12H), 7.11-7.08 (m, 12H), 6.95 (s, 4H, CH_3-C_6H_2), 6.79-6.75 (m, 8H), 5.29 (s, 4H, $CHPh_2$), 5.15 (s, 2H, HC=CH), 2.26 (s, 6H, CH_3-C_6H_2). ^{13}C{^{1}H} NMR (22°C, 126 MHz, CD_2Cl_2): δ 197.9, 195.9, 144.6, 143.6, 142.0, 139.5, 137.5, 130.8, 130.3, 129.9, 128.7, 128.6, 127.1, 126.9, 123.6, 52.2, 22.0. IR (CaF_2/Fluorolube): 2048, 1968 cm^{-1}. Anal. Calcd. for $C_{73}H_{60}N_2NiO_3$: C, 81.90%; H, 5.35%; N, 2.65%. Found: C, 81.60%; H, 5.31%; N = 2.20%.

Reaction of 2 with H_2C=CH_2. A solution of **2** (140 mg, 0.108 mmol in 10 mL toluene) was placed in a sealable reaction flask. The vessel was purged with ethene for 3 minutes before being sealed and removed from light. Addition of ethene caused incorporation of the slurry into solution and a color change to dark brown. After 12 hours the solution was homogenous and orange. Solvent was removed under vacuum and the resulting solid extracted with 10 mL pentane. Filtration of the extract through celite followed by evaporation of solvent under reduced pressure yielded (dmp)NHCH=CH_2 (**5**) in 76% yield as a colorless solid. Sealed ^{1}H-NMR studies conducted under identical conditions show formation of **5** in ~95% yield. ^{13}C NMR data acquired with doubly labeled $^{13}CH_2$=$^{13}CH_2$ ethylene, (IPr*)Ni{N(dmp)$^{13}CH_2{}^{13}CH_2$} (**4-^{13}C**).

For **4**: ^{1}H NMR (22°C, 500 MHz, C_6D_6): δ 7.50 (d, 8H, J = 7.5 Hz, Ar*), 7.11 (t, 8H, J = 7.5 Hz, Ar*), 7.04 (t, 4H, J = 7.5 Hz, p-C_6H_5), 6.82-6.76 (m, 12H, Ar*), 6.73 (d, 8H, 7.5 Hz, Ar*), 6.62 (s, 4H, C_6H_2), 6.51 (s, 4H, -$CHPh_2$), 5.17 (s, 2H, CH=CH), 3.34 (t, 2H, J = 7.0 Hz, NiNCH_2CH_2), 2.22 (s, 12H, Mes), 2.07 (s, 6H), 2.05 (s, 6H), 0.62 (t, 2H, J = 7.0 Hz, NiNCH_2CH_2). ^{13}C NMR for **4-^{13}C** (126 MHz, Tol-d_8, 0°C): δ 54.84 (dt, $^1J_{C\text{-}H}$ = 137 Hz, $^1J_{C\text{-}C}$ = 35.4 Hz, -^{13}CH_2Ndmp), -13.53 (dt, $^1J_{C\text{-}H}$ = 145 Hz, $^1J_{C\text{-}C}$ = 35.4 Hz, -^{13}CH_2Ni).

For **5**: ^{1}H NMR (22°C, 500 MHz, C_6D_6): δ 7.21 (d, 2H, J = 5.9 Hz, C_6H_3), 7.19 (t, 1H, J = 5.9 Hz, C_6H_3), 7.18 (s, 4H, C_6H_2), 6.44 (ddd, 1H, $J_{H\text{-}NH}$ = 11.5 Hz, $J_{H\text{-}H}$ = 14.8 Hz, $J_{H\text{-}H}$ = 8.2 Hz, C=CH-N), 5.79 (d, 1H, J = 11.5 Hz, -NHdmp), 3.96 (d, 1H, J = 14.8 Hz, H_2C=C), 3.79 (d, 1H, J = 8.2 Hz, H_2C=C), 2.48 (s, 6H, p-Mes_{dmp}), 2.47 (s, 12H, m-Mes_{dmp}). ^{13}C NMR for **5-^{13}C** (126 MHz, Tol-d_8, 22°C): δ 135.7 (d d t, $^{1}J_{C\text{-}H}$ = 170 Hz, $^{1}J_{C\text{-}C}$ = 75.7 Hz, $^{2}J_{C\text{-}H}$ = 4.0 Hz, ^{13}CH-NH), 87.26 (d d d t, $^{1}J_{C\text{-}H}$ = 163 Hz, $^{1}J_{C\text{-}H}$ = 153 Hz, $^{1}J_{C\text{-}C}$ = 75.7 Hz, $^{2}J_{C\text{-}H}$ = 3.0 Hz, =^{13}CH_2). GC-MS (m/z) = 355.2 (M^+), 340.4.

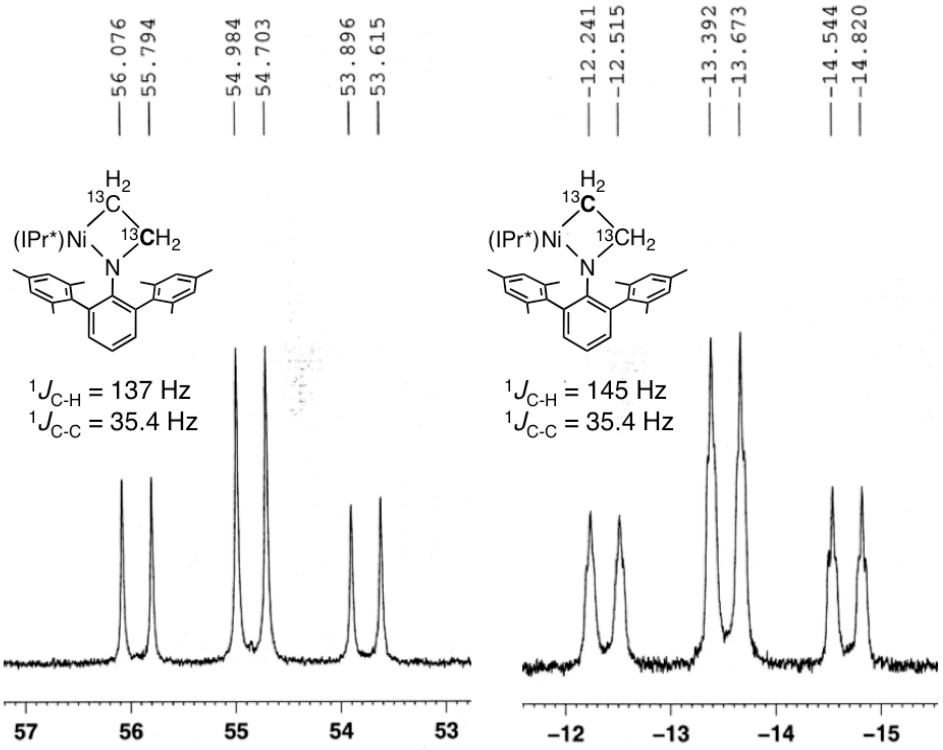

^{13}C NMR of (IPr*)Ni{N(dmp)^{13}$CH_2^{13}CH_2$} (**4-^{13}C**)in Tol-d_8 (22°C, 126 MHz).

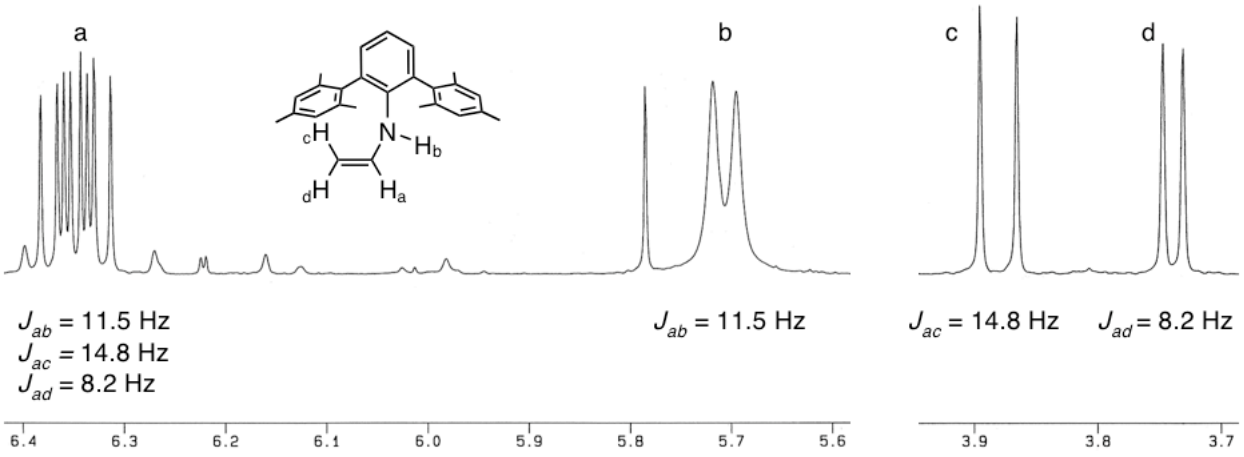

^{1}H NMR of **5** in C_6D_6 (22°C, 500 MHz).

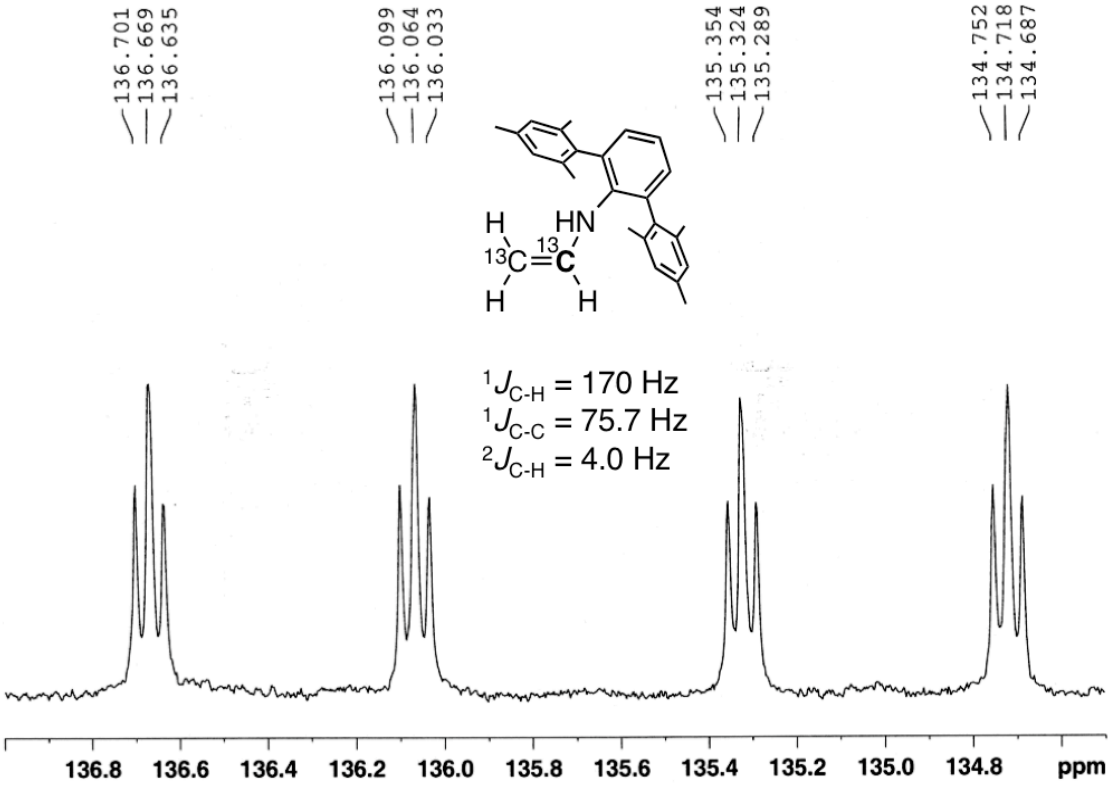

^{13}C NMR of **5-^{13}C** in Tol-d_8 (22°C, 126 MHz).

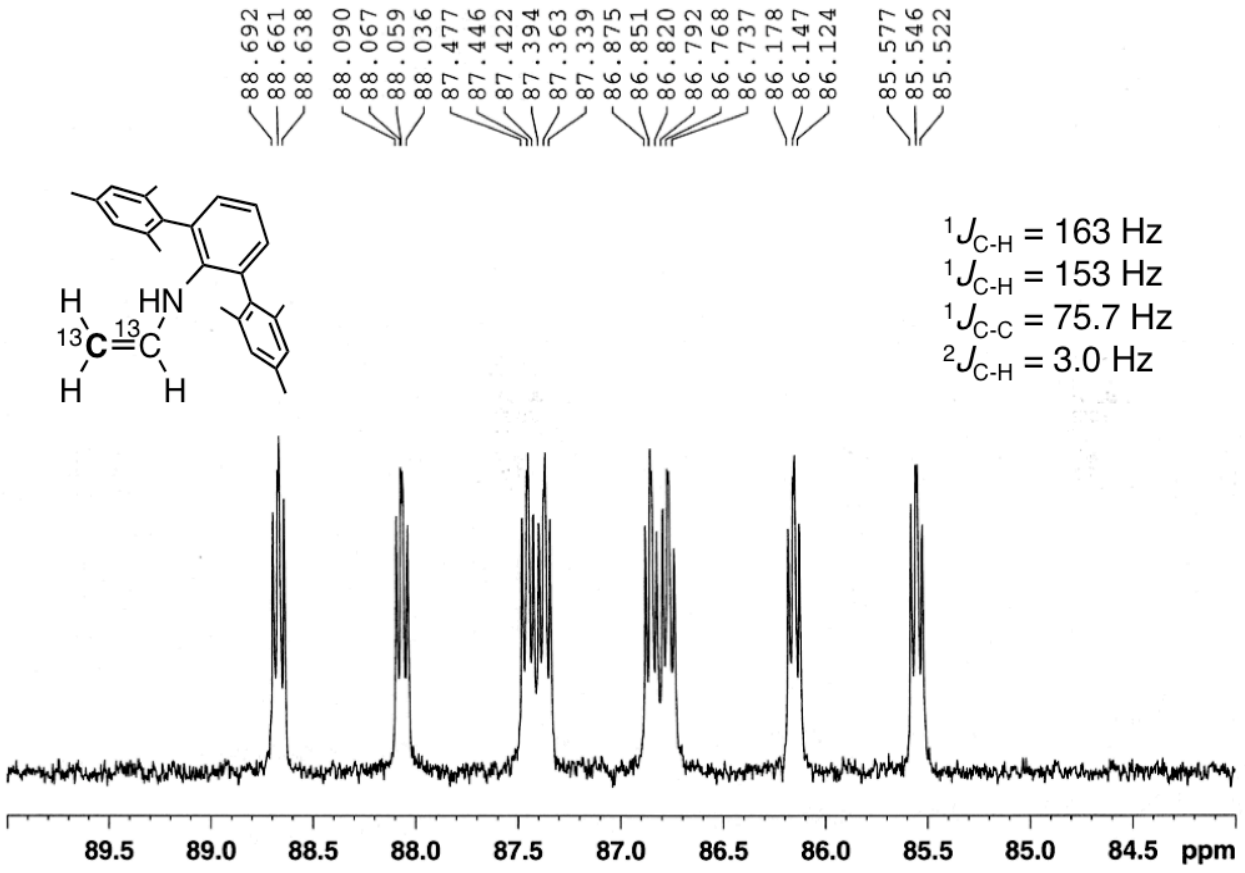

^{13}C NMR of **5-^{13}C** in Tol-d_8 (22°C, 126 MHz).

(IPr*)Ni(η^2-CH_2=CH_2)$_2$ (**6**). Complex **1** (36 mg, mmol) was placed in a Teflon-sealed NMR tube with 1.3 mL C_6D_6. The NMR tube was purged with CH_2CH_2 for 5 minutes. Agitation of the solution caused an immediate change in color from cherry-red to orange-yellow. Attempts to isolate **6** were hampered by facile replacement of the CH_2CH_2 ligands with solvent when placed under reduced pressure. Single crystals suitable for X-ray were collected from a concentrated toluene solution in presence of excess CH_2=CH_2.

For **6**: ^{1}H NMR (22°C, 500 MHz, C_6D_6): δ 7.30 (d, 8H, J = 7.7 Hz, Ar*), 7.05 (t, 8H, J = 7.6 Hz, Ar*), 6.97 (d, 12H, 7.5 Hz, Ar*), 6.93 (s, 4H, C_6H_2), 6.87 (t, 8H, J = 7.7 Hz, Ar*), 6.34 (s, 4H, -$CHPh_2$), 5.55 (s, 2H, CH=CH), 3.00 (s, 8H, CH_2=CH_2), 1.69 (s, 6H, p-CH_3). ^{13}C{^{1}H} NMR (22°C, 126 MHz, C_6D_6): δ 202.3, 144.9, 144.1, 141.8, 138.2, 130.9, 130.2, 129.7, 128.6, 128.5, 126.7, 126.6, 51.67, 49.47.

(II) SQUID Measurements

Measurements were recorded using a Quantum Designs SQUID magnetometer running Magnetic Property Measurement System Revision 2 software. Data were recorded at 5000 and 50,000 G (0.5 and 5 T). A gel cap was charged with 46.0 mg of a powder sample and loaded into a clear plastic straw in a nitrogen-filled glove box. The loaded sample was immediately submerged in liquid nitrogen upon removal from the box, and held under nitrogen until insertion into the magnetometer. The sample was centered within the magnetometer using the DC centering scan at 35 K and 5000 G. Data were acquired from 4-28 K (one data point every 2 K), 30-150 K (one data point every 5 K), and 160-300 K (one data point every 10 K). The magnetic susceptibility was adjusted for underlying diamagnetic contributions using the constitutive corrections of Pascal's constants. The molar magnetic susceptibility (χ_m) was calculated by converting the calculated magnetic susceptibility (χ) obtained from the magnetometer to a molar susceptibility using the multiplication factor: molecular weight/[sample weight*field strength]. Curie-Weiss behavior was determined by plotting χ_m^{-1} vs. T. The effective magnetic moment was calculated using eq 1.

$$\mu_{\text{eff}} = (7.997\chi_m T)^{1/2} \qquad (1)$$

Simulations of magnetic susceptibility were carried out using the JulX program (version 1.4.1), written by Eckhard Bill (*4*). Variables used to fit the data were g, D, and Temperature-Independent Paramagnetism (TIP). Simulation (red lines in plots) of the 0.5 T data provided a gyromagnetic ratio g = 1.96, zero-field splitting parameter D = 24 cm^{-1}, and TIP value, -129.1 x 10^{-6} emu. Neither intermolecular interactions (Weiss temperature, Θ) nor impurities were considered in the simulation. The g value leads to a new expected effective moment: $\mu_{\text{eff}} = g$ x $(S(S+1))^{1/2}$ = 2.78 μ_B, which agrees well with the experimentally observed value of 2.77 μ_B. A separate simulation was carried out for the variable-temperature/variable-field plot (VTVF). Despite slight differences observed at different fields (μ_{eff} varied by ~0.04-0.09 μ_B, probably due to a minor impurity), the data was fit reasonably well: the magnitude of the field dependence is consistent with a positive value of D and a significant zero-field splitting term. Similar parameters were obtained for the two-field simulation: g = 1.96, D = 26 cm^{-1}, TIP = -234 x 10^{-6} emu. Taken together, the magnetic susceptibility data suggest a magnetically isolated S = 1

species with a significant zero-field splitting term (~25 cm^{-1} between the m_s = 0 and m_s = -1, 1 states).

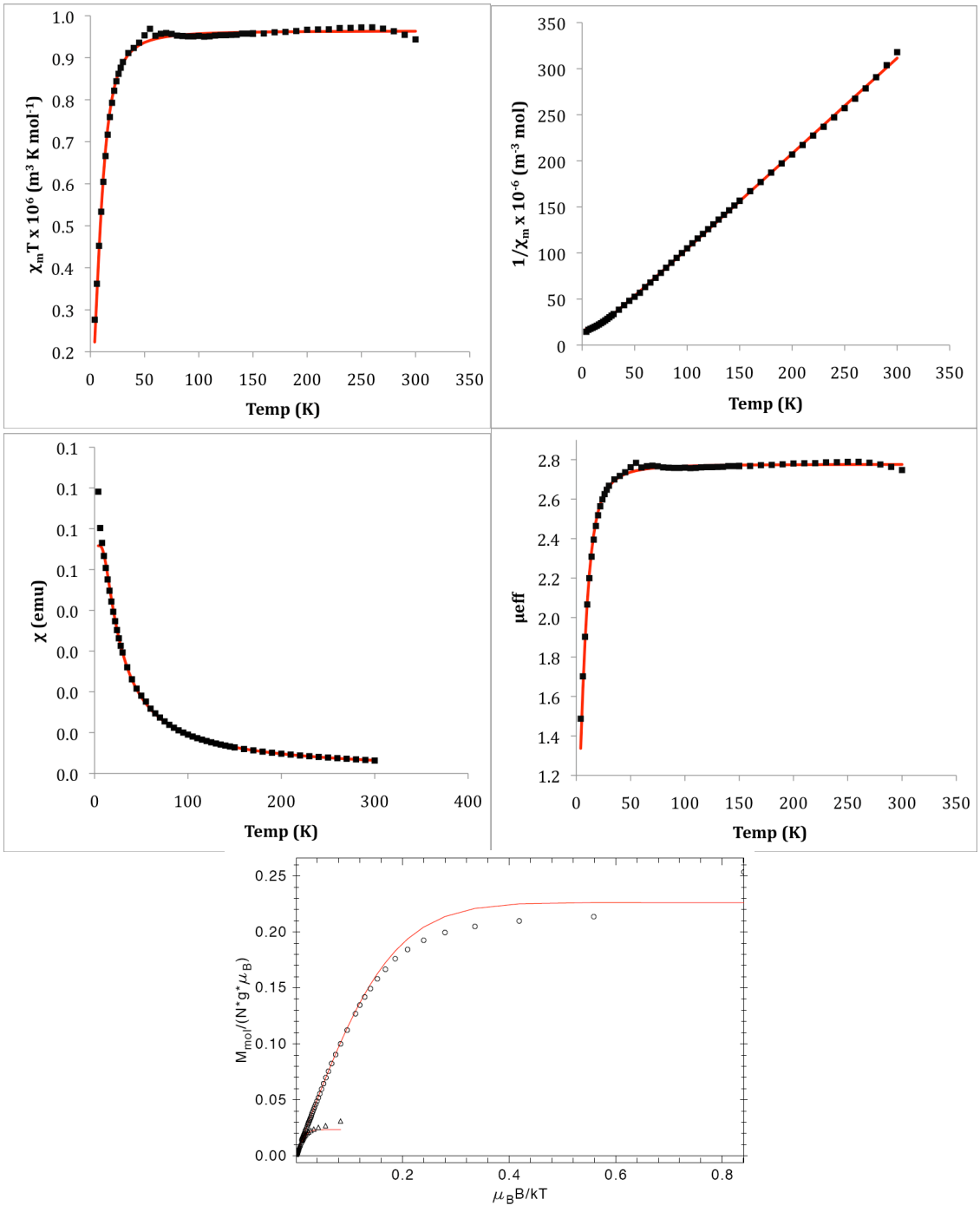

(III) X-Ray Studies

X-Ray Structure Determination. A crystal of suitable size and appearance was selected under a stereo-microscope while immersed in Paratone-N oil to minimize exposure to air. The crystal was extracted from the oil using a tapered glass filament that also held the crystal during data collection. The crystal was mounted and aligned on a Bruker SMART APEX system. All images showed sharp diffractions. Frames separated in reciprocal space were collected and provided an orientation matrix and initial cell parameters. The full data set provided final cell parameters.

A hemisphere of data was obtained at 100 K in reciprocal space to a resolution of 0.84 Å using 0.3° steps in ω using integration times of 10-30 s per frame, depending on the sample. Integration of intensities and refinement of cell parameters were completed with SAINT. Absorption corrections were applied using SADABS or psi-scans and were small. Crystals showed no visual signs of decomposition after data collection.

(IPr*)(THF)NiCl$_2$. The space group was determined as Fdd2 based on systematic absences and intensity statistics. Direct methods were used to refine Ni, C, Cl, N, and O atoms. All atoms were converted to and refined anisotropically. All non-hydrogen atoms were converted to and refined anisotropically. All hydrogen atoms were refined isotropically and fixed at calculated positions. A coordinated molecule of THF is bisected by a rotation axis and displays limited disorder.

Crystal data and structure refinement for (IPr*)(THF)NiCl$_2$:

Identification code	carl134a	Index ranges	-20<=h<=12
Empirical formula	C_{89} H_{86} Cl_2 N_2 Ni O_5		-32<=k<=33
Formula weight	1393.21		-33<=l<=34
Temperature	100(2) K	Reflections collected	18144
Wavelength	0.71073 Å	Independent reflections	6295 [R(int) = 0.0661]
Crystal system	Orthorhombic	Completeness to theta = 25.00°	100.0 %
Space group	Fdd2	Absorption correction	Semi-empirical from equivalents
Unit cell dimensions	a = 17.515(3) Å		
	b = 28.008(4) Å	Max. and min. transmission	0.9242 and 0.7952
	c = 29.362(4) Å	Refinement method	Full-matrix least-squares on F^2
	a= 90°		
	b= 90°	Data / restraints / parameters	6295 / 1 / 448
	g = 90°	Goodness-of-fit on F^2	0.991
Volume	14403(3) $Å^3$	Final R indices [I>2sigma(I)]	R1 = 0.0722
Z	8		wR2 = 0.1743
Density (calculated)	1.285 Mg/m^3	R indices (all data)	R1 = 0.0951
Absorption coefficient	0.400 mm^{-1}		wR2 = 0.1849
F(000)	5888	Absolute structure parameter	0.01(3)
Crystal size	0.60 x 0.20 x 0.20 mm^3	Largest diff. peak and hole	0.629 and -0.405 e.$Å^{-3}$
Theta range for data collection	1.54 to 25.00°.		

Fully labeled ORTEP (35%) of (IPr*)(THF)$NiCl_2$. A crystallographic rotation axis bisects the molecule, one half is displayed (left):

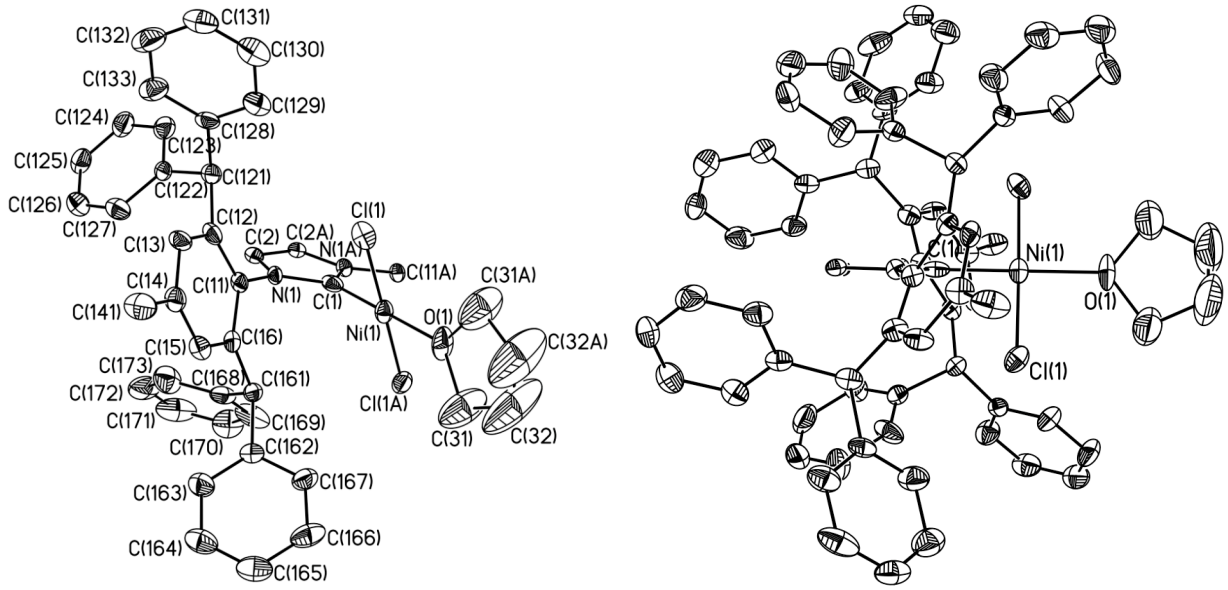

Bond Distances (Å) for (IPr*)(THF)$NiCl_2$:

Ni(1)-C(1)	1.859(10)	O(1)-C(31)#1	1.500(12)	C(132)-C(133)	1.375(10)
Ni(1)-O(1)	1.967(6)	O(1)-C(31)	1.500(12)	C(131)-C(130)	1.296(11)
Ni(1)-Cl(1)#1	2.1732(14)	C(161)-C(168)	1.531(8)	C(162)-C(163)	1.348(8)
Ni(1)-Cl(1)	2.1732(14)	C(161)-C(162)	1.539(7)	C(162)-C(167)	1.364(8)
C(1)-N(1)	1.365(7)	C(121)-C(122)	1.531(8)	C(163)-C(164)	1.387(9)
C(1)-N(1)#1	1.365(7)	C(121)-C(128)	1.544(8)	C(164)-C(165)	1.353(10)
N(1)-C(2)	1.402(7)	C(122)-C(123)	1.373(8)	C(167)-C(166)	1.376(9)
N(1)-C(11)	1.457(6)	C(122)-C(127)	1.382(8)	C(170)-C(171)	1.346(13)
C(16)-C(15)	1.405(7)	C(128)-C(129)	1.341(9)	C(170)-C(169)	1.372(10)
C(16)-C(11)	1.438(7)	C(128)-C(133)	1.386(9)	C(168)-C(169)	1.377(10)
C(16)-C(161)	1.489(7)	C(2)-C(2)#1	1.333(10)	C(168)-C(173)	1.381(10)
C(15)-C(14)	1.359(8)	C(124)-C(125)	1.362(9)	C(172)-C(171)	1.367(13)
C(11)-C(12)	1.377(8)	C(124)-C(123)	1.414(9)	C(172)-C(173)	1.410(12)
C(13)-C(12)	1.401(8)	C(125)-C(126)	1.375(10)	C(165)-C(166)	1.386(11)
C(13)-C(14)	1.419(8)	C(127)-C(126)	1.396(10)	C(31)-C(32)	1.470(17)
C(14)-C(141)	1.510(8)	C(129)-C(130)	1.434(10)	C(32)-C(32)#1	1.14(3)
C(12)-C(121)	1.540(8)	C(132)-C(131)	1.361(11)		

Bond Angles (°) for (IPr*)(THF)$NiCl_2$:

C(1)-Ni(1)-O(1)	180.0	N(1)#1-C(1)-Ni(1)	127.8(4)	C(12)-C(11)-C(16)	122.6(4)
C(1)-Ni(1)-Cl(1)#1	89.48(5)	C(1)-N(1)-C(2)	110.8(5)	C(12)-C(11)-N(1)	120.2(4)
O(1)-Ni(1)-Cl(1)#1	90.52(5)	C(1)-N(1)-C(11)	125.2(5)	C(16)-C(11)-N(1)	117.2(4)
C(1)-Ni(1)-Cl(1)	89.48(5)	C(2)-N(1)-C(11)	123.9(4)	C(12)-C(13)-C(14)	121.1(5)
O(1)-Ni(1)-Cl(1)	90.52(5)	C(15)-C(16)-C(11)	115.1(5)	C(15)-C(14)-C(13)	118.1(5)
Cl(1)#1-Ni(1)-Cl(1)	178.96(10)	C(15)-C(16)-C(161)	122.8(5)	C(15)-C(14)-C(141)	122.8(5)
N(1)-C(1)-N(1)#1	104.3(7)	C(11)-C(16)-C(161)	122.0(4)	C(13)-C(14)-C(141)	119.0(6)
N(1)-C(1)-Ni(1)	127.8(4)	C(14)-C(15)-C(16)	124.2(5)	C(11)-C(12)-C(13)	118.3(5)

C(11)-C(12)-C(121)	123.0(5)	C(133)-C(128)-C(121)	122.4(6)	C(165)-C(164)-C(163)	121.3(7)
C(13)-C(12)-C(121)	118.6(5)	C(2)#1-C(2)-N(1)	107.1(3)	C(162)-C(167)-C(166)	121.9(6)
C(31)#1-O(1)-C(31)	104.2(10)	C(125)-C(124)-C(123)	120.6(6)	C(171)-C(170)-C(169)	118.2(8)
C(31)#1-O(1)-Ni(1)	127.9(5)	C(122)-C(123)-C(124)	120.5(6)	C(169)-C(168)-C(173)	119.9(6)
C(31)-O(1)-Ni(1)	127.9(5)	C(124)-C(125)-C(126)	119.1(6)	C(169)-C(168)-C(161)	117.9(6)
C(16)-C(161)-C(168)	112.2(4)	C(122)-C(127)-C(126)	120.9(6)	C(173)-C(168)-C(161)	122.2(6)
C(16)-C(161)-C(162)	115.4(4)	C(125)-C(126)-C(127)	120.4(6)	C(170)-C(169)-C(168)	121.3(8)
C(168)-C(161)-C(162)	110.7(4)	C(128)-C(129)-C(130)	119.6(7)	C(171)-C(172)-C(173)	118.3(8)
C(122)-C(121)-C(12)	112.2(4)	C(131)-C(132)-C(133)	119.1(7)	C(168)-C(173)-C(172)	118.9(8)
C(122)-C(121)-C(128)	111.4(5)	C(130)-C(131)-C(132)	120.7(7)	C(164)-C(165)-C(166)	117.2(7)
C(12)-C(121)-C(128)	111.1(4)	C(132)-C(133)-C(128)	121.8(7)	C(167)-C(166)-C(165)	120.5(7)
C(123)-C(122)-C(127)	118.3(6)	C(131)-C(130)-C(129)	121.1(7)	C(170)-C(171)-C(172)	123.3(8)
C(123)-C(122)-C(121)	118.6(5)	C(163)-C(162)-C(167)	117.3(5)	C(32)-C(31)-O(1)	103.1(10)
C(127)-C(122)-C(121)	123.1(5)	C(163)-C(162)-C(161)	123.7(5)	C(32)#1-C(32)-C(31)	114.2(7)
C(129)-C(128)-C(133)	117.7(6)	C(167)-C(162)-C(161)	119.0(5)		
C(129)-C(128)-C(121)	119.7(6)	C(162)-C(163)-C(164)	121.7(6)		

(IPr*)Ni=N(dmp) (**2**). The space group was determined as P2(1)/c based on systematic absences and intensity statistics. Direct methods were used to refine Ni, C, N, and O atoms (co-crystallized Et_2O). All atoms were converted to and refined anisotropically. All non-hydrogen atoms were converted to and refined anisotropically. All hydrogen atoms were refined isotropically and fixed at calculated positions.

Crystal data and structure refinement for (IPr*)Ni=N(dmp) (**2**):

Identification code	carl150a	Theta range for data collection	1.21 to 25.00°.
Empirical formula	C_{97} H_{91} N_3 Ni O	Index ranges	-15<=h<=15
Formula weight	1373.44		-28<=k<=28
Temperature	100(2) K		-28<=l<=28
Wavelength	0.71073 Å	Reflections collected	74570
Crystal system	Monoclinic	Independent reflections	13272 [R(int) =
Space group	P2(1)/c	0.1364]	
Unit cell dimensions	a = 13.3746(10) Å	Completeness to theta = 25.00°	99.9 %
	b = 24.1618(18) Å	Absorption correction	Psi-scan
	c = 23.9714(18) Å	Max. and min. transmission	0.9407 and 0.8361
	a= 90°	Refinement method	Full-matrix least-
	b= 103.287(2)°		squares on F^2
	g = 90°	Data / restraints / parameters	13272 / 0 / 929
Volume	7539.1(10) $Å^3$	Goodness-of-fit on F^2	0.925
Z	4	Final R indices [I>2sigma(I)]	R1 = 0.0553
Density (calculated)	1.210 Mg/m^3		wR2 = 0.0843
Absorption coefficient	0.310 mm^{-1}	R indices (all data)	R1 = 0.1080
F(000)	2920		wR2 = 0.0910
Crystal size	0.60 x 0.20 x 0.20 mm^3	Largest diff. peak and hole	0.741 and -0.639 e.$Å^{-3}$

Fully labeled ORTEP (35%) of (IPr*)Ni=N(dmp) (**2**). The molecule is separated into two halves for clarity:

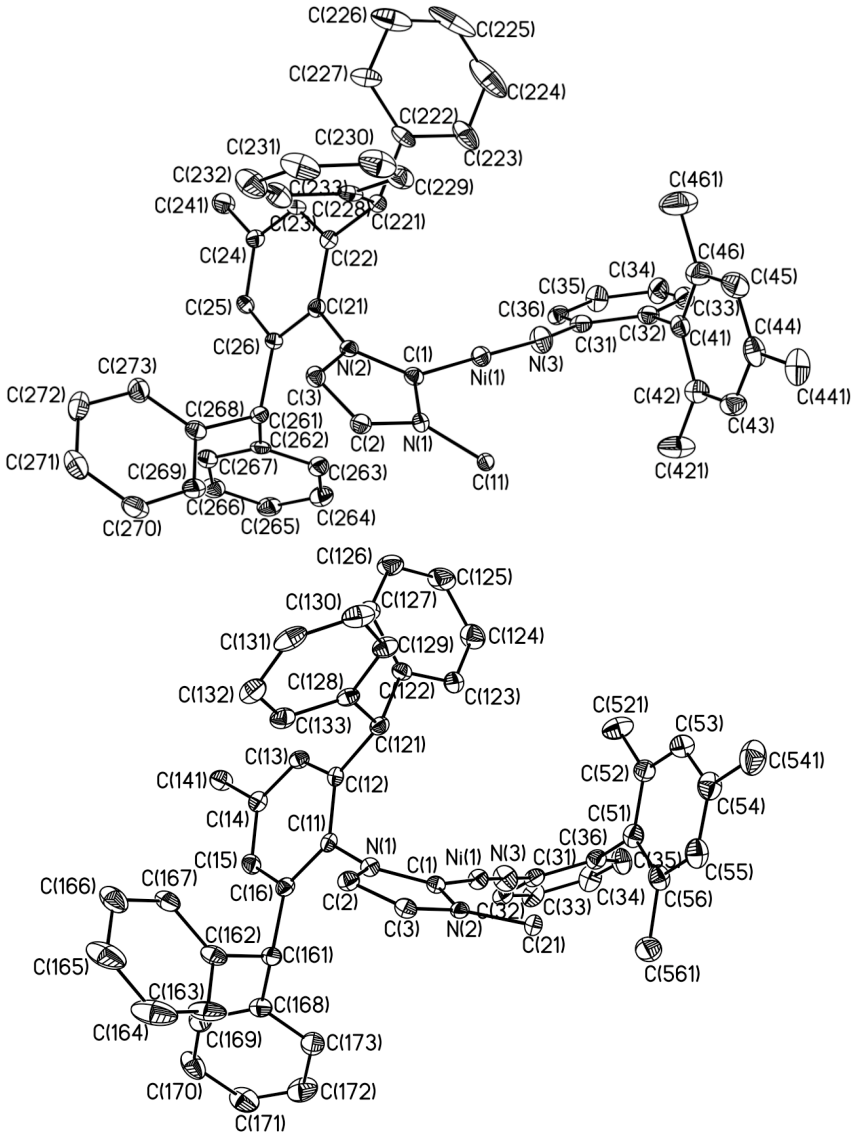

Bond Distances (Å) for (IPr*)Ni=N(dmp) (**2**):

Ni(1)-N(3)	1.663(3)	C(12)-C(13)	1.377(4)	C(24)-C(25)	1.392(4)
Ni(1)-C(1)	1.917(3)	C(12)-C(121)	1.522(4)	C(24)-C(241)	1.503(4)
C(1)-N(1)	1.353(3)	C(13)-C(14)	1.390(4)	C(25)-C(26)	1.383(4)
C(1)-N(2)	1.381(3)	C(14)-C(15)	1.392(4)	C(26)-C(261)	1.529(4)
N(1)-C(2)	1.380(3)	C(14)-C(141)	1.503(4)	C(31)-C(36)	1.414(4)
N(1)-C(11)	1.442(3)	C(15)-C(16)	1.395(4)	C(31)-C(32)	1.444(4)
N(2)-C(3)	1.382(3)	C(16)-C(161)	1.523(4)	C(32)-C(33)	1.380(4)
N(2)-C(21)	1.442(3)	C(21)-C(22)	1.387(4)	C(32)-C(41)	1.486(4)
C(2)-C(3)	1.338(4)	C(21)-C(26)	1.397(4)	C(33)-C(34)	1.376(4)
N(3)-C(31)	1.351(4)	C(22)-C(23)	1.388(4)	C(34)-C(35)	1.385(4)
C(11)-C(16)	1.398(4)	C(22)-C(221)	1.523(4)	C(35)-C(36)	1.375(4)
C(11)-C(12)	1.402(4)	C(23)-C(24)	1.385(4)	C(36)-C(51)	1.500(4)

C(41)-C(46)	1.388(4)	C(126)-C(127)	1.383(4)	C(223)-C(224)	1.368(5)
C(41)-C(42)	1.398(4)	C(128)-C(129)	1.385(4)	C(224)-C(225)	1.357(6)
C(42)-C(43)	1.385(4)	C(128)-C(133)	1.388(4)	C(225)-C(226)	1.372(5)
C(42)-C(421)	1.504(4)	C(129)-C(130)	1.374(4)	C(226)-C(227)	1.389(4)
C(43)-C(44)	1.379(4)	C(130)-C(131)	1.377(4)	C(228)-C(233)	1.376(4)
C(44)-C(45)	1.374(4)	C(131)-C(132)	1.374(4)	C(228)-C(229)	1.379(4)
C(44)-C(441)	1.507(4)	C(132)-C(133)	1.395(4)	C(229)-C(230)	1.390(4)
C(45)-C(46)	1.376(4)	C(161)-C(168)	1.518(4)	C(230)-C(231)	1.377(4)
C(46)-C(461)	1.515(4)	C(161)-C(162)	1.529(4)	C(231)-C(232)	1.367(4)
C(51)-C(56)	1.392(4)	C(162)-C(167)	1.378(4)	C(232)-C(233)	1.396(4)
C(51)-C(52)	1.397(4)	C(162)-C(163)	1.392(4)	C(261)-C(268)	1.524(4)
C(52)-C(53)	1.391(4)	C(163)-C(164)	1.361(4)	C(261)-C(262)	1.531(4)
C(52)-C(521)	1.495(4)	C(164)-C(165)	1.370(5)	C(262)-C(267)	1.377(4)
C(53)-C(54)	1.390(4)	C(165)-C(166)	1.370(5)	C(262)-C(263)	1.381(4)
C(54)-C(55)	1.380(4)	C(166)-C(167)	1.384(4)	C(263)-C(264)	1.390(4)
C(54)-C(541)	1.499(4)	C(168)-C(169)	1.376(4)	C(264)-C(265)	1.373(4)
C(55)-C(56)	1.379(4)	C(168)-C(173)	1.388(4)	C(265)-C(266)	1.375(4)
C(56)-C(561)	1.512(4)	C(169)-C(170)	1.390(4)	C(266)-C(267)	1.392(4)
C(121)-C(122)	1.520(4)	C(170)-C(171)	1.373(4)	C(268)-C(273)	1.376(4)
C(121)-C(128)	1.521(4)	C(171)-C(172)	1.349(4)	C(268)-C(269)	1.386(4)
C(122)-C(123)	1.383(4)	C(172)-C(173)	1.393(4)	C(269)-C(270)	1.368(4)
C(122)-C(127)	1.393(4)	C(221)-C(222)	1.522(4)	C(270)-C(271)	1.368(4)
C(123)-C(124)	1.379(4)	C(221)-C(228)	1.525(4)	C(271)-C(272)	1.372(4)
C(124)-C(125)	1.376(4)	C(222)-C(227)	1.372(4)	C(272)-C(273)	1.390(4)
C(125)-C(126)	1.377(4)	C(222)-C(223)	1.384(4)		

Bond Angles (°) for (IPr*)Ni=N(dmp) (**2**):

N(3)-Ni(1)-C(1)	174.24(13)	C(21)-C(22)-C(23)	116.6(3)	C(45)-C(44)-C(43)	117.1(3)
N(1)-C(1)-N(2)	103.6(2)	C(21)-C(22)-C(221)	120.7(3)	C(45)-C(44)-C(441)	122.1(3)
N(1)-C(1)-Ni(1)	125.3(2)	C(23)-C(22)-C(221)	122.7(3)	C(43)-C(44)-C(441)	120.8(3)
N(2)-C(1)-Ni(1)	131.0(2)	C(24)-C(23)-C(22)	122.7(3)	C(44)-C(45)-C(46)	122.8(3)
C(1)-N(1)-C(2)	111.9(3)	C(23)-C(24)-C(25)	118.4(3)	C(45)-C(46)-C(41)	119.6(3)
C(1)-N(1)-C(11)	121.1(2)	C(23)-C(24)-C(241)	121.1(3)	C(45)-C(46)-C(461)	120.2(3)
C(2)-N(1)-C(11)	126.8(3)	C(25)-C(24)-C(241)	120.5(3)	C(41)-C(46)-C(461)	120.2(3)
C(1)-N(2)-C(3)	110.3(2)	C(26)-C(25)-C(24)	121.6(3)	C(56)-C(51)-C(52)	119.6(3)
C(1)-N(2)-C(21)	124.2(2)	C(25)-C(26)-C(21)	117.5(3)	C(56)-C(51)-C(36)	121.5(3)
C(3)-N(2)-C(21)	124.6(2)	C(25)-C(26)-C(261)	121.2(3)	C(52)-C(51)-C(36)	118.9(3)
C(3)-C(2)-N(1)	106.6(3)	C(21)-C(26)-C(261)	121.3(3)	C(53)-C(52)-C(51)	118.6(3)
C(31)-N(3)-Ni(1)	171.6(3)	N(3)-C(31)-C(36)	121.1(3)	C(53)-C(52)-C(521)	120.3(3)
C(2)-C(3)-N(2)	107.5(3)	N(3)-C(31)-C(32)	120.7(3)	C(51)-C(52)-C(521)	121.0(3)
C(16)-C(11)-C(12)	122.6(3)	C(36)-C(31)-C(32)	118.2(3)	C(54)-C(53)-C(52)	122.4(3)
C(16)-C(11)-N(1)	118.1(3)	C(33)-C(32)-C(31)	118.9(3)	C(55)-C(54)-C(53)	117.4(3)
C(12)-C(11)-N(1)	119.2(3)	C(33)-C(32)-C(41)	120.2(3)	C(55)-C(54)-C(541)	120.7(3)
C(13)-C(12)-C(11)	116.8(3)	C(31)-C(32)-C(41)	120.9(3)	C(53)-C(54)-C(541)	121.9(3)
C(13)-C(12)-C(121)	122.1(3)	C(34)-C(33)-C(32)	122.3(3)	C(56)-C(55)-C(54)	122.0(3)
C(11)-C(12)-C(121)	120.9(3)	C(33)-C(34)-C(35)	118.6(3)	C(55)-C(56)-C(51)	119.9(3)
C(12)-C(13)-C(14)	123.0(3)	C(36)-C(35)-C(34)	122.3(3)	C(55)-C(56)-C(561)	119.9(3)
C(13)-C(14)-C(15)	118.6(3)	C(35)-C(36)-C(31)	119.7(3)	C(51)-C(56)-C(561)	120.1(3)
C(13)-C(14)-C(141)	121.1(3)	C(35)-C(36)-C(51)	120.4(3)	C(122)-C(121)-C(128)	112.5(2)
C(15)-C(14)-C(141)	120.4(3)	C(31)-C(36)-C(51)	119.9(3)	C(122)-C(121)-C(12)	112.2(2)
C(14)-C(15)-C(16)	121.1(3)	C(46)-C(41)-C(42)	118.8(3)	C(128)-C(121)-C(12)	113.4(2)
C(15)-C(16)-C(11)	117.8(3)	C(46)-C(41)-C(32)	121.5(3)	C(123)-C(122)-C(127)	118.2(3)
C(15)-C(16)-C(161)	121.5(3)	C(42)-C(41)-C(32)	119.7(3)	C(123)-C(122)-C(121)	120.2(3)
C(11)-C(16)-C(161)	120.5(3)	C(43)-C(42)-C(41)	119.6(3)	C(127)-C(122)-C(121)	121.6(3)
C(22)-C(21)-C(26)	123.2(3)	C(43)-C(42)-C(421)	119.9(3)	C(124)-C(123)-C(122)	121.2(3)
C(22)-C(21)-N(2)	119.8(3)	C(41)-C(42)-C(421)	120.5(3)	C(125)-C(124)-C(123)	120.1(3)
C(26)-C(21)-N(2)	117.0(3)	C(44)-C(43)-C(42)	122.1(3)	C(124)-C(125)-C(126)	119.6(3)

C(125)-C(126)-C(127)	120.4(3)	C(173)-C(168)-C(161)	119.6(3)	C(231)-C(232)-C(233)	120.2(3)
C(126)-C(127)-C(122)	120.5(3)	C(168)-C(169)-C(170)	121.5(3)	C(228)-C(233)-C(232)	120.6(3)
C(129)-C(128)-C(133)	117.4(3)	C(171)-C(170)-C(169)	119.2(3)	C(268)-C(261)-C(26)	111.9(2)
C(129)-C(128)-C(121)	119.8(3)	C(172)-C(171)-C(170)	120.6(4)	C(268)-C(261)-C(262)	114.0(2)
C(133)-C(128)-C(121)	122.8(3)	C(171)-C(172)-C(173)	120.5(4)	C(26)-C(261)-C(262)	113.0(2)
C(130)-C(129)-C(128)	121.8(3)	C(168)-C(173)-C(172)	120.3(3)	C(267)-C(262)-C(263)	118.9(3)
C(129)-C(130)-C(131)	120.5(3)	C(222)-C(221)-C(22)	114.1(2)	C(267)-C(262)-C(261)	123.6(3)
C(132)-C(131)-C(130)	119.0(3)	C(222)-C(221)-C(228)	110.2(2)	C(263)-C(262)-C(261)	117.5(3)
C(131)-C(132)-C(133)	120.5(3)	C(22)-C(221)-C(228)	114.3(2)	C(262)-C(263)-C(264)	121.0(3)
C(128)-C(133)-C(132)	120.8(3)	C(227)-C(222)-C(223)	119.0(3)	C(265)-C(264)-C(263)	119.6(3)
C(168)-C(161)-C(16)	114.0(3)	C(227)-C(222)-C(221)	121.8(3)	C(264)-C(265)-C(266)	119.9(3)
C(168)-C(161)-C(162)	113.1(3)	C(223)-C(222)-C(221)	119.1(3)	C(265)-C(266)-C(267)	120.3(3)
C(16)-C(161)-C(162)	110.9(3)	C(224)-C(223)-C(222)	120.1(4)	C(262)-C(267)-C(266)	120.2(3)
C(167)-C(162)-C(163)	117.6(3)	C(225)-C(224)-C(223)	121.2(4)	C(273)-C(268)-C(269)	117.7(3)
C(167)-C(162)-C(161)	123.3(3)	C(224)-C(225)-C(226)	119.4(4)	C(273)-C(268)-C(261)	123.5(3)
C(163)-C(162)-C(161)	118.9(3)	C(225)-C(226)-C(227)	120.1(4)	C(269)-C(268)-C(261)	118.7(3)
C(164)-C(163)-C(162)	121.3(4)	C(222)-C(227)-C(226)	120.1(4)	C(270)-C(269)-C(268)	122.3(3)
C(163)-C(164)-C(165)	120.4(4)	C(233)-C(228)-C(229)	118.6(3)	C(269)-C(270)-C(271)	119.2(3)
C(166)-C(165)-C(164)	119.8(4)	C(233)-C(228)-C(221)	122.9(3)	C(270)-C(271)-C(272)	120.3(3)
C(165)-C(166)-C(167)	119.8(4)	C(229)-C(228)-C(221)	118.4(3)	C(271)-C(272)-C(273)	120.1(3)
C(162)-C(167)-C(166)	121.1(3)	C(228)-C(229)-C(230)	120.9(3)	C(268)-C(273)-C(272)	120.5(3)
C(169)-C(168)-C(173)	118.0(3)	C(231)-C(230)-C(229)	119.9(3)		
C(169)-C(168)-C(161)	122.5(3)	C(232)-C(231)-C(230)	119.7(3)		

(IPr*)Ni(η^2-CH_2=CH_2)$_2$ (**6**). The space group was determined as P-1 based on systematic absences and intensity statistics. Patterson method was used to locate the Ni atom. Direct methods were used to refine Ni, C, and N. All atoms were converted to and refined anisotropically. All non-hydrogen atoms were converted to and refined anisotropically. All hydrogen atoms were refined isotropically and fixed at calculated positions.

Crystal data and structure refinement for (IPr*)Ni(η^2-CH_2=CH_2)$_2$ (**6**):

Identification code	carl170a	Theta range for data collection	1.83 to 25.00°.
Empirical formula	C_{87} H_{80} N_2 Ni	Index ranges	-13<=h<=13
Formula weight	1212.24		-19<=k<=19
Temperature	100(2) K		-23<=l<=23
Wavelength	0.71073 Å	Reflections collected	32689
Crystal system	Triclinic	Independent reflections	11703 [R(int) =
Space group	P-1	0.0392]	
Unit cell dimensions	a = 10.9750(6) Å	Completeness to theta = 25.00°	99.8 %
	b = 16.0260(9) Å	Absorption correction	Psi-scan
	c = 19.3760(11) Å	Max. and min. transmission	0.9352 and 0.8222
	a= 79.0740(10)°	Refinement method	Full-matrix least-
	b= 85.0950(10)°		squares on F^2
	g = 89.2870(10)°	Data / restraints / parameters	11703 / 0 / 815
Volume	3333.9(3) $Å^3$	Goodness-of-fit on F^2	1.097
Z	2	Final R indices [I>2sigma(I)]	R1 = 0.0360
Density (calculated)	1.208 Mg/m^3		wR2 = 0.0967
Absorption coefficient	0.340 mm^{-1}	R indices (all data)	R1 = 0.0410
F(000)	1288		wR2 = 0.0988
Crystal size	0.60 x 0.20 x 0.20 mm^3	Largest diff. peak and hole	0.517 and -0.223 e.$Å^{-3}$

Fully labeled ORTEP (35%) of (IPr*)Ni(η^2-CH_2=CH_2)$_2$ (**6**). The molecule is separated into two halves for clarity:

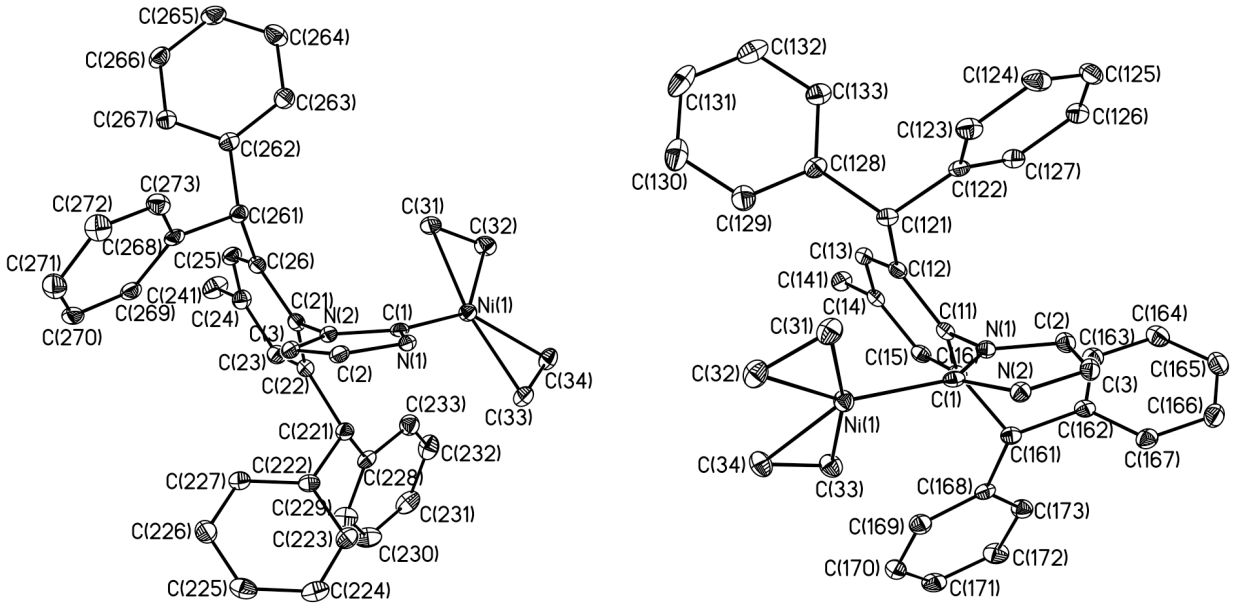

Bond Distances (Å) for (IPr*)Ni(η^2-CH_2=CH_2)$_2$ (**6**):

Ni(1)-C(1)	1.9116(15)	C(122)-C(123)	1.389(2)	C(269)-C(270)	1.386(2)
Ni(1)-C(32)	1.9803(15)	C(122)-C(121)	1.525(2)	C(269)-C(268)	1.391(2)
Ni(1)-C(34)	1.9845(15)	C(130)-C(131)	1.383(3)	C(267)-C(266)	1.385(2)
Ni(1)-C(33)	1.9873(15)	C(133)-C(132)	1.390(2)	C(261)-C(268)	1.530(2)
Ni(1)-C(31)	1.9964(15)	C(168)-C(173)	1.386(2)	C(266)-C(265)	1.380(2)
C(1)-N(2)	1.3731(19)	C(168)-C(169)	1.390(2)	C(271)-C(270)	1.381(2)
C(1)-N(1)	1.3786(18)	C(168)-C(161)	1.537(2)	C(271)-C(272)	1.391(2)
N(1)-C(2)	1.3889(18)	C(161)-C(162)	1.525(2)	C(273)-C(272)	1.379(2)
N(1)-C(11)	1.4431(19)	C(162)-C(163)	1.386(2)	C(273)-C(268)	1.391(2)
N(2)-C(3)	1.3957(18)	C(162)-C(167)	1.394(2)	C(264)-C(265)	1.385(2)
N(2)-C(21)	1.4440(18)	C(167)-C(166)	1.385(2)	C(228)-C(229)	1.382(2)
C(2)-C(3)	1.333(2)	C(165)-C(166)	1.380(2)	C(228)-C(233)	1.390(2)
C(16)-C(15)	1.396(2)	C(165)-C(164)	1.381(2)	C(228)-C(221)	1.526(2)
C(16)-C(11)	1.401(2)	C(169)-C(170)	1.379(2)	C(222)-C(227)	1.389(2)
C(16)-C(161)	1.532(2)	C(163)-C(164)	1.388(2)	C(222)-C(223)	1.395(2)
C(15)-C(14)	1.383(2)	C(170)-C(171)	1.381(2)	C(222)-C(221)	1.524(2)
C(14)-C(13)	1.393(2)	C(173)-C(172)	1.391(2)	C(225)-C(226)	1.377(2)
C(14)-C(141)	1.509(2)	C(26)-C(21)	1.395(2)	C(225)-C(224)	1.379(2)
C(13)-C(12)	1.383(2)	C(26)-C(25)	1.396(2)	C(223)-C(224)	1.382(2)
C(11)-C(12)	1.404(2)	C(26)-C(261)	1.525(2)	C(226)-C(227)	1.390(2)
C(12)-C(121)	1.525(2)	C(22)-C(23)	1.390(2)	C(229)-C(230)	1.392(2)
C(129)-C(130)	1.383(2)	C(22)-C(21)	1.405(2)	C(233)-C(232)	1.388(2)
C(129)-C(128)	1.387(2)	C(22)-C(221)	1.522(2)	C(33)-C(34)	1.391(2)
C(128)-C(133)	1.389(2)	C(24)-C(25)	1.382(2)	C(31)-C(32)	1.393(2)
C(128)-C(121)	1.524(2)	C(24)-C(23)	1.395(2)	C(132)-C(131)	1.376(3)
C(126)-C(125)	1.376(2)	C(24)-C(241)	1.504(2)	C(231)-C(230)	1.374(3)
C(126)-C(127)	1.393(2)	C(263)-C(262)	1.386(2)	C(231)-C(232)	1.380(3)
C(125)-C(124)	1.383(2)	C(263)-C(264)	1.387(2)	C(171)-C(172)	1.379(2)
C(124)-C(123)	1.381(2)	C(262)-C(267)	1.387(2)		
C(122)-C(127)	1.387(2)	C(262)-C(261)	1.526(2)		

Bond Angles (°) for (IPr*)Ni(η^2-CH_2=CH_2)$_2$ (**6**):

C(1)-Ni(1)-C(32)	138.21(6)	C(123)-C(122)-C(121)	118.56(14)	C(267)-C(262)-C(261)	121.51(14)
C(1)-Ni(1)-C(34)	136.46(6)	C(128)-C(121)-C(12)	113.00(12)	C(270)-C(269)-C(268)	120.62(16)
C(32)-Ni(1)-C(34)	85.30(7)	C(128)-C(121)-C(122)	111.93(12)	C(266)-C(267)-C(262)	121.08(15)
C(1)-Ni(1)-C(33)	95.51(6)	C(12)-C(121)-C(122)	112.45(12)	C(26)-C(261)-C(262)	112.54(12)
C(32)-Ni(1)-C(33)	126.28(7)	C(124)-C(123)-C(122)	121.13(16)	C(26)-C(261)-C(268)	111.58(12)
C(34)-Ni(1)-C(33)	41.00(6)	C(122)-C(127)-C(126)	120.60(15)	C(262)-C(261)-C(268)	111.28(12)
C(1)-Ni(1)-C(31)	97.27(6)	C(129)-C(130)-C(131)	120.16(17)	C(265)-C(266)-C(267)	120.09(16)
C(32)-Ni(1)-C(31)	41.00(6)	C(128)-C(133)-C(132)	120.61(16)	C(270)-C(271)-C(272)	119.21(16)
C(34)-Ni(1)-C(31)	126.27(7)	C(173)-C(168)-C(169)	117.92(14)	C(272)-C(273)-C(268)	121.16(16)
C(33)-Ni(1)-C(31)	167.06(6)	C(173)-C(168)-C(161)	122.81(14)	C(265)-C(264)-C(263)	120.17(16)
N(2)-C(1)-N(1)	102.54(12)	C(169)-C(168)-C(161)	119.26(14)	C(273)-C(268)-C(269)	118.30(15)
N(2)-C(1)-Ni(1)	128.15(11)	C(162)-C(161)-C(16)	111.10(12)	C(273)-C(268)-C(261)	118.58(14)
N(1)-C(1)-Ni(1)	129.31(11)	C(162)-C(161)-C(168)	111.92(12)	C(269)-C(268)-C(261)	123.07(14)
C(1)-N(1)-C(2)	111.69(12)	C(16)-C(161)-C(168)	111.39(12)	C(273)-C(272)-C(271)	120.12(17)
C(1)-N(1)-C(11)	125.74(12)	C(163)-C(162)-C(167)	118.25(14)	C(271)-C(270)-C(269)	120.53(16)
C(2)-N(1)-C(11)	122.54(12)	C(163)-C(162)-C(161)	121.87(14)	C(266)-C(265)-C(264)	119.47(15)
C(1)-N(2)-C(3)	111.80(12)	C(167)-C(162)-C(161)	119.86(14)	C(229)-C(228)-C(233)	118.20(15)
C(1)-N(2)-C(21)	124.80(12)	C(166)-C(167)-C(162)	120.78(16)	C(229)-C(228)-C(221)	123.24(15)
C(3)-N(2)-C(21)	123.34(12)	C(166)-C(165)-C(164)	119.42(16)	C(233)-C(228)-C(221)	118.56(14)
C(3)-C(2)-N(1)	107.19(13)	C(170)-C(169)-C(168)	121.38(15)	C(227)-C(222)-C(223)	118.19(15)
C(15)-C(16)-C(11)	117.56(13)	C(162)-C(163)-C(164)	120.90(15)	C(227)-C(222)-C(221)	122.91(14)
C(15)-C(16)-C(161)	119.83(13)	C(165)-C(164)-C(163)	120.25(16)	C(223)-C(222)-C(221)	118.89(14)
C(11)-C(16)-C(161)	122.58(13)	C(165)-C(166)-C(167)	120.39(16)	C(226)-C(225)-C(224)	119.74(16)
C(14)-C(15)-C(16)	122.70(14)	C(169)-C(170)-C(171)	120.21(16)	C(224)-C(223)-C(222)	120.93(15)
C(15)-C(14)-C(13)	118.01(14)	C(168)-C(173)-C(172)	120.74(15)	C(225)-C(226)-C(227)	120.22(16)
C(15)-C(14)-C(141)	121.31(13)	C(2)-C(3)-N(2)	106.76(13)	C(225)-C(224)-C(223)	120.20(16)
C(13)-C(14)-C(141)	120.67(13)	C(21)-C(26)-C(25)	118.06(14)	C(222)-C(227)-C(226)	120.70(15)
C(12)-C(13)-C(14)	121.93(14)	C(21)-C(26)-C(261)	122.02(13)	C(22)-C(221)-C(222)	112.31(12)
C(16)-C(11)-C(12)	121.18(13)	C(25)-C(26)-C(261)	119.83(13)	C(22)-C(221)-C(228)	113.04(12)
C(16)-C(11)-N(1)	119.32(13)	C(23)-C(22)-C(21)	118.26(14)	C(222)-C(221)-C(228)	113.38(13)
C(12)-C(11)-N(1)	119.46(12)	C(23)-C(22)-C(221)	121.45(14)	C(228)-C(229)-C(230)	120.77(17)
C(13)-C(12)-C(11)	118.59(13)	C(21)-C(22)-C(221)	120.25(13)	C(232)-C(233)-C(228)	121.18(17)
C(13)-C(12)-C(121)	121.45(13)	C(25)-C(24)-C(23)	117.87(14)	C(34)-C(33)-Ni(1)	69.39(9)
C(11)-C(12)-C(121)	119.90(13)	C(25)-C(24)-C(241)	120.54(14)	C(32)-C(31)-Ni(1)	68.88(9)
C(130)-C(129)-C(128)	120.96(17)	C(23)-C(24)-C(241)	121.59(15)	C(31)-C(32)-Ni(1)	70.12(9)
C(129)-C(128)-C(133)	118.41(15)	C(24)-C(25)-C(26)	122.54(15)	C(33)-C(34)-Ni(1)	69.61(9)
C(129)-C(128)-C(121)	119.39(14)	C(22)-C(23)-C(24)	122.06(15)	C(131)-C(132)-C(133)	120.27(17)
C(133)-C(128)-C(121)	122.19(14)	C(26)-C(21)-C(22)	121.14(14)	C(132)-C(131)-C(130)	119.57(17)
C(125)-C(126)-C(127)	120.32(16)	C(26)-C(21)-N(2)	119.32(13)	C(230)-C(231)-C(232)	119.79(17)
C(126)-C(125)-C(124)	119.52(15)	C(22)-C(21)-N(2)	119.54(13)	C(231)-C(232)-C(233)	119.75(17)
C(123)-C(124)-C(125)	120.12(16)	C(262)-C(263)-C(264)	120.79(15)	C(231)-C(230)-C(229)	120.31(17)
C(127)-C(122)-C(123)	118.30(14)	C(263)-C(262)-C(267)	118.40(14)	C(172)-C(171)-C(170)	119.22(15)
C(127)-C(122)-C(121)	123.12(14)	C(263)-C(262)-C(261)	120.07(14)	C(171)-C(172)-C(173)	120.47(16)

(IV) Computational Methods

All simulations employed the Gaussian 09 suite of programs (*5*). Initial single point calculations on the imido complex **2** at its X-ray geometry indicated a triplet state as being significantly lower in energy than singlet and quintet states, consistent with the experimental magnetic measurements, and so further computational analyses focused on this multiplicity. Calculations utilized the unrestricted (S = 1) Kohn-Sham formalism.

Experimental X-ray coordinates for (IPr*)Ni=Ndmp (**2**) were used as the starting point for the geometry optimization of the full complex and a truncated model, (NHC)Ni=NPh, NHC = parent N-heterocyclic carbene ligand. The latter was used to provide a C_{2v} geometry to facilitate orbital analysis. Both full and truncated models gave near identical core geometries: Ni-N_{imide} = 1.69 Å, Ni-$C_{carbene}$ = 1.94 Å, C_{ipso}-N_{imide} = 1.33 Å (truncated model of **2**); Ni-N_{imide} = 1.69 Å, Ni-$C_{carbene}$ = 1.94 Å, C_{ipso}-N_{imide} = 1.34 Å (full model of **2**).

For the truncated model, the level of theory employed was B3LYP/6-311+G(d). For the full model of **2**, a hybrid QM/MM approach was used within the ONIOM (*6*) formalism. The substituents on the IPr* nitrogens and the 2,6-mesityl substituents on the imide ligand were modeled with the UFF (*7*) force field while the remainder of **2** was modeled at the B3LYP/6-311+G(d) level of theory.

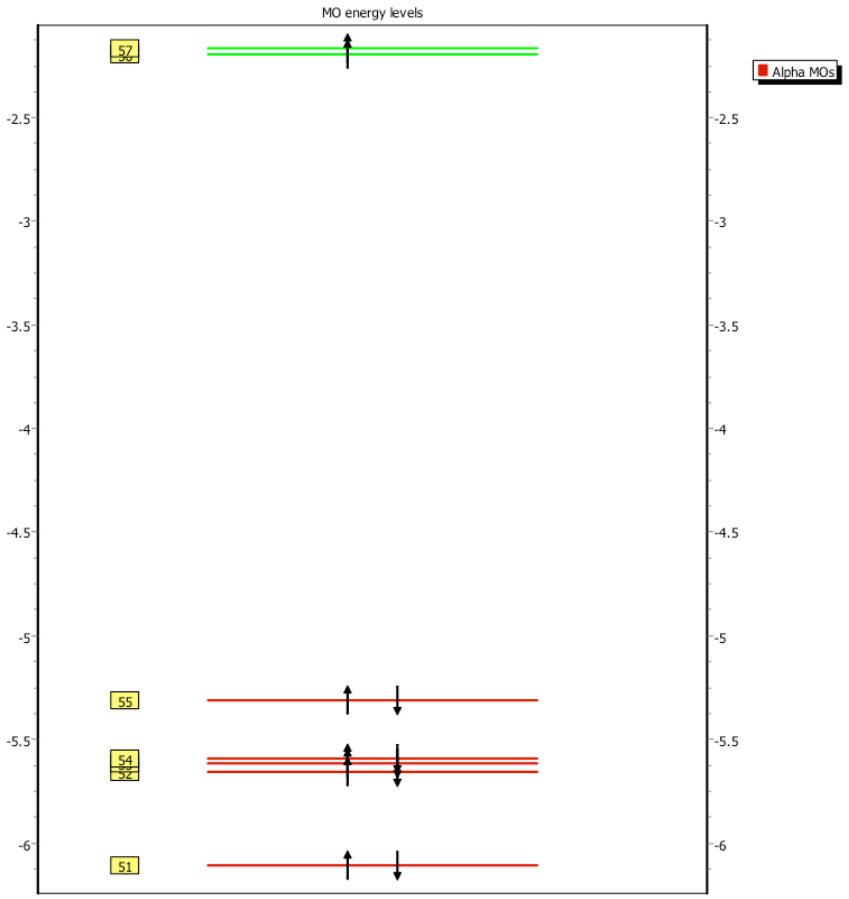

Frontier Kohn Sham orbitals (B3LYP/6-311+G(d)) using the restricted open-shell DFT formalism. Energy scale is in eV.

57	-2.17	b_1
56	-2.20	b_2
55	-5.31	a_1
54	-5.59	a_2
53	-5.61	b_1
52	-5.66	a_1
51	-6.11	b_2

Orbital energies (eV) for frontier orbitals in MO diagram above and which are depicted below.

NiN π_y – MO 51 – b_2

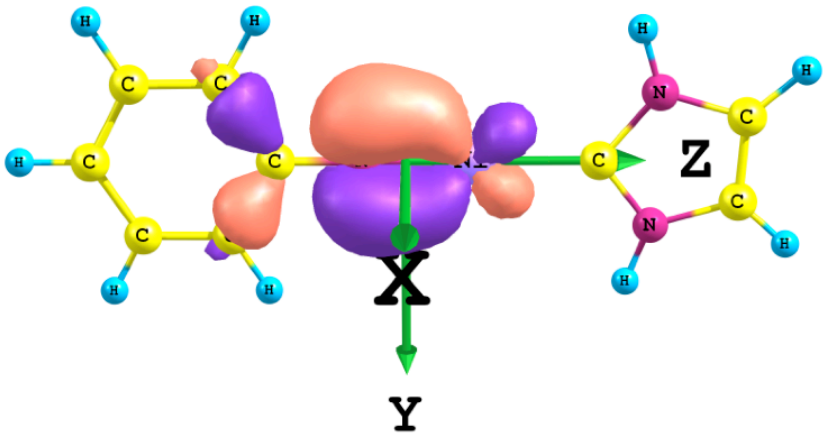

Ni ($\delta + \sigma$) – MO 52 – a_1

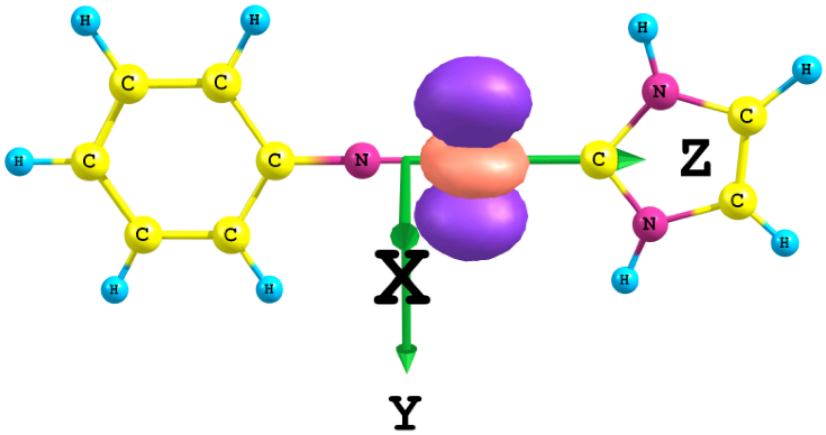

NiN π_x - MO 53 – b_1

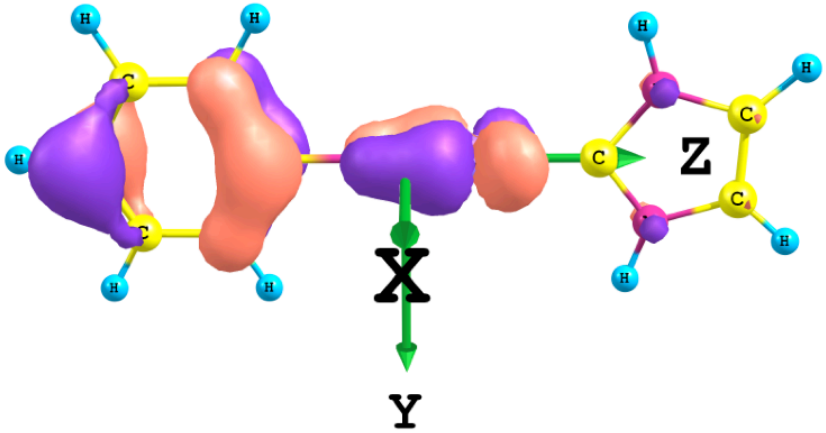

Ni δ – MO54 – a_2

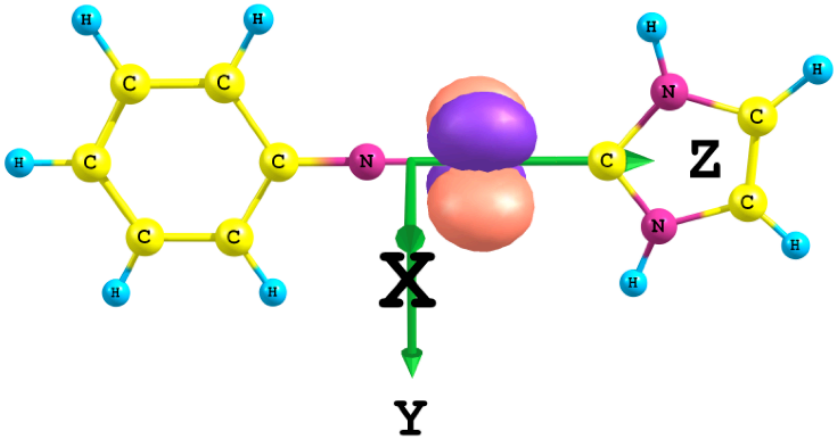

Ni (δ + σ) – MO 55 – a_1

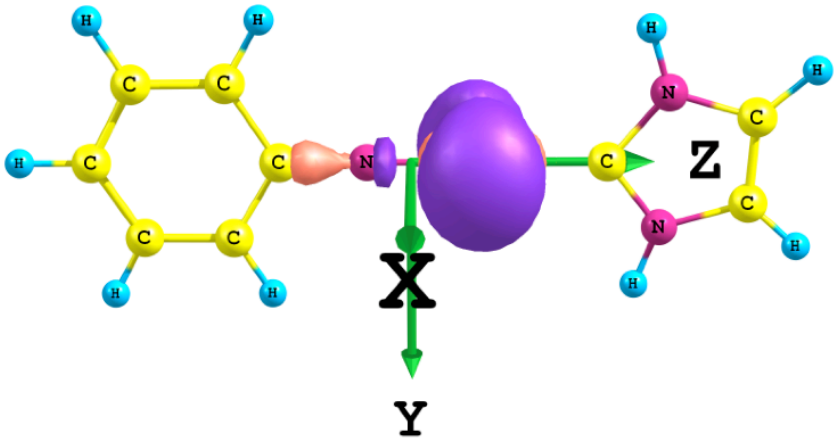

NiN π^*_x – MO 56 – b_2

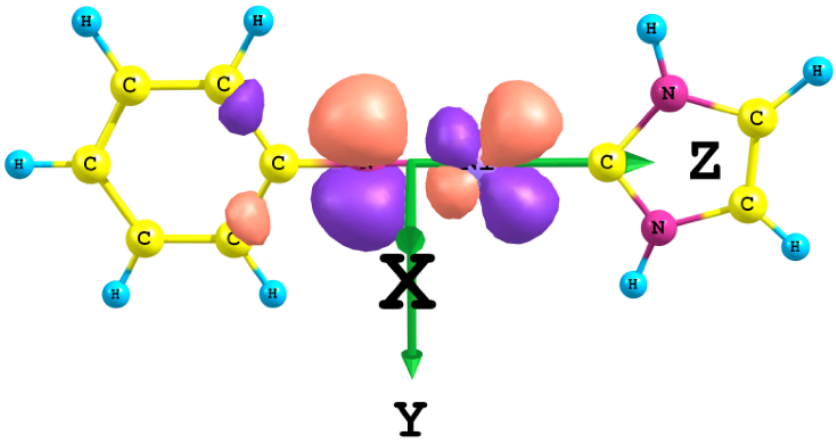

NiN π^*_x – MO 57 – b_1

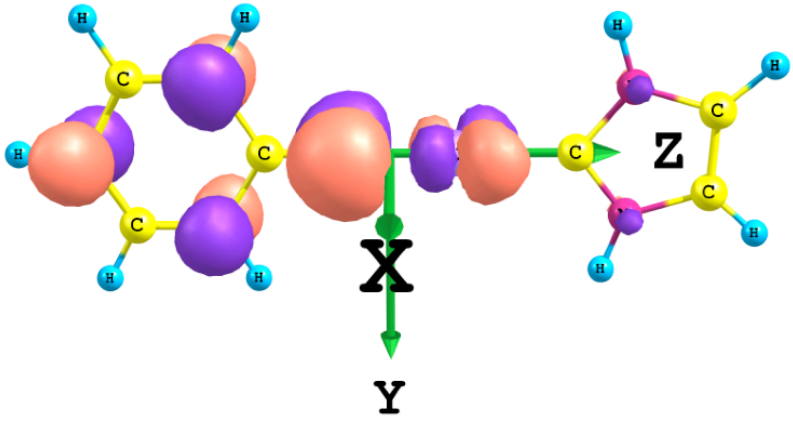

For the C2v model, NHC-Ni=NPh, the molecular plane is the yz plane. The orbitals are plotted from the same point of view, slightly off the x-axis.

(V) References

1. For a general description of air-sensitive techniques and equipment, see: Burger, B. J.; Bercaw, J. E. in *Experimental Organometallic Chemistry*; Wayda, A. L.; Darensbourg, M. Y. Eds.; ACS Symposium Series 357, American Chemical Society; Washington, DC. **1987**; pp 79-89.
2. Berthon-Gelloz, G.; Siegler, M. A.; Spek, A. L.; Tinant, B.; Reek, J. N. H.; Markó, I. E. *Dalton Trans.* **2010**, *6*, 1444.
3. Gavennois, J.; Tilley, T. D. *Organometallics* **2002**, *21*, 5549.
4. Bill, E. *JulX 1.4, A Program for the Simulation and Analysis of Magnetic Suseptibility Data*; Max Plank Institute for Bioinorganic Chemistry: Mülheim an der Ruhr, 2008.
5. Gaussian 09, Revision **A.1**, M. J. Frisch, G. W. Trucks, H. B. Schlegel, G. E. Scuseria, M. A. Robb, J. R. Cheeseman, G. Scalmani, V. Barone, B. Mennucci, G. A. Petersson, H. Nakatsuji, M. Caricato, X. Li, H. P. Hratchian, A. F. Izmaylov, J. Bloino, G. Zheng, J. L. Sonnenberg, M. Hada, M. Ehara, K. Toyota, R. Fukuda, J. Hasegawa, M. Ishida, T. Nakajima, Y. Honda, O. Kitao, H. Nakai, T. Vreven, J. A. Montgomery, Jr., J. E. Peralta, F. Ogliaro, M. Bearpark, J. J. Heyd, E. Brothers, K. N. Kudin, V. N. Staroverov, R. Kobayashi, J. Normand, K. Raghavachari, A. Rendell, J. C. Burant, S. S. Iyengar, J. Tomasi, M. Cossi, N. Rega, J. M. Millam, M. Klene, J. E. Knox, J. B. Cross, V. Bakken, C. Adamo, J.

Jaramillo, R. Gomperts, R. E. Stratmann, O. Yazyev, A. J. Austin, R. Cammi, C. Pomelli, J. W. Ochterski, R. L. Martin, K. Morokuma, V. G. Zakrzewski, G. A. Voth, P. Salvador, J. J. Dannenberg, S. Dapprich, A. D. Daniels, Ö. Farkas, J. B. Foresman, J. V. Ortiz, J. Cioslowski, D. J. Fox, Gaussian, Inc., Wallingford CT, 2009.

6. Svensson, M.; Humbel, S.; Froese, R. D. J.; Matsubara, T.; Sieber, S.; Morokuma, K.; *J. Phys. Chem.* **1996**, *100***,** 19357.
7. Rappé, A. K.; Casewit, C. J.; Colwell, K. S.; Goddard III, W. A.; Skiff, W. M. *J. Am. Chem. Soc.* **1992**, *114*, 10024.